Fractional-PD^{μ} Controllers for Implicitly Defined Systems

A.-J. Guel-Cortez[1], Mihir Sen[2], C.-F. Méndez-Barrios[1] and Bill Goodwine[2]

***Abstract*— This work presents a simple procedure for designing fractional PD^{μ} controllers for a type of implicit operators, which have recently been studied to describe large-scale systems. The methodology developed proposes a geometrical approach that allows characterizing the parameter-space of the PD^{μ} controller into stable and unstable regions. Several numerical examples illustrate the effectiveness of the proposed results.**

I. Introduction

Implicit operators are integro-differential operators that instead of being explicilty defined are solutions of an operator equation [1], [2]. Fractional derivatives of rational order are special cases for this type of operator [1]. In [2], the total operator describing the potential-driven flow dynamics in a large-scale self-similar tree network is implicitly defined. A problem with this definition is the lack of obvious meaning in the time-domain, but in the Laplace-domain we may study its significance. In [3] a self-similar infinite tree network of springs and dampers is studied in the Laplace domain to obtain an expression relating the position of the last elements with the first element in the tree. We call this type of model an implicitly defined transfer function (IDTF). In the same manner, an infinite ladder of mass-springs and dampers is studied in [4] presenting again this type of relationship. In addition, similar transfer functions can be found when solving partial differential equations (for further details, see [5], [6]). Hence, infinite dimensional order systems can be modeled by using these kind of expressions (for instance, see [5], [7], [8]).

PID control is one of the most popular control strategies, especially for industrial purposes [9]. It is said that the study of classical *PID* controllers is already mature. Nonetheless, in recent years due to the explosion of fractional calculus applications the use of *PID* controllers using a fractional derivative D^{μ} and integral I^{λ} have been studied extensively in different applications (see [10]–[13]). These type of controllers are proven to provide better results when applied to fractional-order systems (see [12]–[16]). Its advantage relies on the use of more degrees of freedom, which is helpful to obtain results that otherwise would be difficult or even impossible to derive [17]. Fractional-PD^{μ} controller design has been studied for linear time invariant systems of integer and for fractional-order systems with time delay (for some examples, see [12], [13]).

In this context, we aim to study the stability of fractional PD^{μ} controllers when applied to IDTF. The analysis will require the use of the *D*-composition method studied in [18], [19] to obtain the (k_p, k_d) parameters regions that stabilizes the IDTF. Additionally, we develop a fragility analysis to obtain a robustness measure of the controller and present some numerical examples.

Throughout the paper the following standard notation is adopted: $\mathbb{C}$ is the set of complex numbers, $\boldsymbol{i} := \sqrt{-1}$, all points in the complex plane whose real part is positive, will be called the right half-plane (RHP), whereas all points whose real part is negative will be called the left half-plane (LHP). Also, for $z \in \mathbb{C}$, $\bar{z}$, $\arg z$, $\Re(z)$ and $\Im(z)$ define the complex conjugate, main argument (i.e., $\arg z \in (-\pi, \pi]$), and the real and imaginary parts of z respectively. $\mathbb{R}$ ($\mathbb{R}_+$ and $\mathbb{R}_-$) denotes the set of real numbers (strictly positive, strictly negative) and $\mathbb{N}$ and $\mathbb{Q}$ denote the set of natural and rational numbers respectively. For $\mathbf{x}, \mathbf{y} \in \mathbb{C}^n$, the scalar product is denoted by $\langle \mathbf{x}, \mathbf{y} \rangle = \mathbf{y}^H \mathbf{x}$, where $\mathbf{y}^H$ is the complex conjugate transpose of $\mathbf{y}$.

II. Preliminary Results

First we review some fundamental definitions and preliminary results that will be useful in the work.

Definition 1 (Branch Point (BP), Branch Cut [20], [21]): A BP is a point such that the function is discontinuous when going around an arbitrarily small circuit around this point. Meanwhile a BC is the union of two BPs by an arbitrary arc. This BC allows access to the $(k+1)^{th}$ sheet from the k^{th} sheet of a Riemann-surface.

Theorem 1 (from [22]): A given multi-valued transfer function is stable if and only if it has no pole in $\mathbb{C}_+$ and no BP in $\mathbb{C}_-$. Here, $\mathbb{C}_+$ and $\mathbb{C}_-$ stand for the closed right half-plane (RHP) and the open RHP of the first Riemann sheet, respectively.

In order to illustrate the importance of Theorem 1, let us consider the following simple IDTF

$$G(s) = \frac{1}{\sqrt{s+k}}, \tag{1}$$

where $k \in \mathbb{R}$. It can be proven that the impulse response of (1) is given by

$$y(t) = \mathscr{L}^{-1}\left[\frac{1}{\sqrt{s+k}}\right] = \frac{e^{-kt}}{\sqrt{\pi t}}. \tag{2}$$

Thus, according to the previous result, the behavior of (2) depends on the location of the BP of (1), which can be found

[1]Guel-Cortez and C.-F. Méndez-Barrios are with Universidad Autónoma de San Luis Potosí (UASLP), Facultad de Ingeniería, Dr. Manuel Nava No. 8, San Luis Potosí, S.L.P., México. adrian.guel@uaslp.mx and cerfranfer@gmail.com.

[2]Bill Goodwine and Mihir Sen are with the Department of Aerospace & Mechanical Engineering, University of Notre Dame, Notre Dame, IN 46556 USA bill@controls.ame.nd.edu and msen@nd.edu.

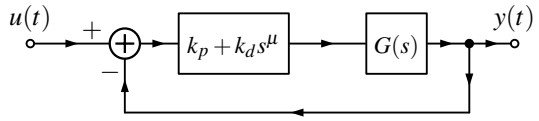

Fig. 1. System to be stabilized.

by solving $s+k=0$. Hence, as Theorem 1 states, when $k<0$ the system is unstable, which is clear from (2).

A. Problem Formulation

Consider the multi-valued transfer function of the form

$$G(s) \quad = \quad \frac{N(s)+\sqrt{\beta_2 s^2+\beta_1 s+\beta_0}}{D(s)+\sqrt{\alpha_2 s^2+\alpha_1 s+\alpha_0}}, \tag{3}$$

where $\alpha_j,\beta_j \in \mathbb{R},\ j\in\{0,1,2\},\ N(s)=\sum_{k=0}^{m} b_k s^k,\ D(s)=\sum_{k=0}^{n} a_k s^k$, a_i, b_i, $a_n \neq 0$ are arbitrary real numbers, and $n \geq m$.

Assumption 1: Polynomials $N(s)$ and $D(s)$ satisfy the following conditions:

(i) $\deg D(s) \geq \deg N(s)$.
(ii) $N(s)$ and $D(s)$ are coprime polynomials.
(iii) $|N(i\omega)|>0,\ \forall \omega \in \mathbb{R}$.
(iv) $D(i\omega^*)=0$, then $|Q'(i\omega^*)|>0$ with $\omega^* \in \mathbb{R}$.

Assumption 2: The functions $P(s) := \sqrt{\beta_2 s^2+\beta_1 s+\beta_0}$ and $Q(s) := \sqrt{\alpha_2 s^2+\alpha_1 s+\alpha_0}$ satisfy the following conditions:

(i) $\deg Q^2(s) \geq \deg P^2(s)$.
(ii) $\alpha_2 \neq a_n$ if $n=2$.
(iii) $Q^2(s_1)=0$ and $P^2(s_2)=0 \iff s_1,s_2 \notin$ RHP.
(iv) if $\deg(D(s))=0$, $\deg Q^2(s) > \deg P^2(s)$.

Problem 1: Derive analytical conditions on the parameters (k_p,k_d,μ) such that the fractional PD^μ controller:

$$C(s)=k_p+k_d s^\mu, \tag{4}$$

BIBO-stabilizes the closed-loop plant in Fig. 1 described by the transfer function in Eq. (3).

Problem 2: For a given $PD^\mu-$controller $\mathbf{k}^*=\left[k_p^*,k_d^*\right]^T \in \mathbb{R}^2$ determine the maximal positive value d, such that the controller (4) stabilizes system (3) for any k_p and k_d, satisfying

$$\sqrt{(k_p-k_d^*)^2+(k_d-k_d^*)^2} < d. \tag{5}$$

III. Main Results

In this section we outline the fractional PD^μ controller restrictions that we will consider in our work. In addition, we give explicit details in the development of the the stability root boundaries of system (3).

A. Controller restrictions

Remark 1: The fractional-order μ is taken as a real number, such that, $\mu \in (0,2)$. Furthermore, $\mu \leq \max(\deg(D(s)), \frac{\deg(Q^2(s))}{2})$, such that, we avoid to increase the system's degree.

Proposition 1: System (3) would be stabilizable by means of the fractional PD^μ controller if and only if $\beta_j \geq 0,\ j \in \{0,1,2\}$.

Remark 2: Proposition 1 claims that our PD^μ controller will not be sufficient to stabilize a system whose BPs are located in RHP. In such a case, a different type of controller must be defined.

B. Stability root boundaries

The closed-loop characteristic equation of system (3) is defined as:

$$\Delta(s) := D(s)+Q(s)+(k_p+k_d s^\mu)(N(s)+P(s)). \tag{6}$$

As mentioned earlier, we are interested in finding the stability regions in the (k_p,k_d)-parameters space when μ is fixed. Hence, the locations of the roots of $\Delta(s)$ will be our main interest. In this vein, the following result and definitions will be useful:

Proposition 2: The poles of the open-loop system are given by the roots of the characteristic equation

$$\tilde{\Delta}(s)=D^2(s)-Q^2(s). \tag{7}$$

Definition 2 (Frequency crossing set): The frequency crossing set $\Omega \subset \mathbb{R}$ is the set of all ω, such that, there exists at least a pair (k_p,k_d) for which

$$Q(i\omega)=D(i\omega)+Q(i\omega)+(k_p+k_d(i\omega)^\mu)(N(i\omega)+P(i\omega))=0. \tag{8}$$

Definition 3 (Stability root boundaries): The stability root boundaries $\mathscr{T}$ is the set of all parameters $(k_p,k_d) \in \mathbb{R}^2$ for which there exists at least one $\omega \in \Omega$, such that, $\Delta(i\omega)=0$. Additionally, any point $\mathbf{k} \in \mathscr{T}$ is known as a crossing point.

C. Stability root boundaries characterization

1) Complex root boundaries (CRB):

Proposition 3: Let $\omega \in \mathbb{R}_+$, then ω is a crossing frequency if and only if $\mathbf{k}(\omega) := [k_p(\omega),k_d(\omega)]^T$, where

$$k_p(\omega) = -\Re\left[\tfrac{D(j\omega)+Q(j\omega)}{N(j\omega)+P(j\omega)}\right]+\Im\left[\tfrac{D(j\omega)+Q(j\omega)}{N(j\omega)+P(j\omega)}\right]\cos\left(\tfrac{\mu\pi}{2}\right) \tag{9}$$

$$k_d(\omega) = -\Im\left[\tfrac{D(j\omega)+Q(j\omega)}{N(j\omega)+P(j\omega)}\right]\omega^{-\mu}\csc\left(\tfrac{\mu\pi}{2}\right). \tag{10}$$

2) Real root boundaries (RRB):

Proposition 4: The crossing through the origin of the complex plane is given by $\mathbf{k}_0$ which is defined as

$$\mathbf{k}_0 := \begin{bmatrix} -\frac{a_0+\sqrt{\alpha_0}}{b_0+\sqrt{\beta_0}} \\ k_d \end{bmatrix}, \tag{11}$$

with $k_d \in \mathbb{R}$.

3) Imaginary root boundaries (IRB):

Proposition 5: Consider the characteristic function $\Delta(s)$, and let $n,m,\tilde{p},\tilde{q}$ be defined as $\deg(D(s))$, $\deg(N(s))$, $\deg(P^2(s))$ and $\deg(Q^2(s))$ respectively. Then, an imaginary root boundary exists if $\mathbf{k}=\mathbf{k}_\infty$, where $\mathbf{k}_\infty$ is given according to the following cases:

(i) $n \geq \frac{\tilde{q}}{2}$

$$\mathbf{k}_\infty = \begin{cases} \begin{bmatrix} k_p \\ -\frac{a_n}{b_m} \end{bmatrix}, k_p \in \mathbb{R} & \text{if} \quad \mu + m = n \\ \begin{bmatrix} k_p \\ -\frac{a_n}{\sqrt{\beta_{\tilde{p}}}} \end{bmatrix}, k_p \in \mathbb{R} & \text{if} \quad \mu + \frac{\tilde{p}}{2} = n \\ \begin{bmatrix} k_p \\ -\frac{a_n}{b_m + \sqrt{\beta_{\tilde{p}}}} \end{bmatrix}, k_p \in \mathbb{R} & \text{if} \quad \mu + m = \mu + \frac{\tilde{p}}{2} = n \end{cases}, \tag{12}$$

(ii) $\frac{\tilde{q}}{2} > n$

$$\mathbf{k}_\infty = \begin{bmatrix} k_p \\ -\frac{\sqrt{\alpha_{\tilde{q}}}}{\sqrt{\beta_{\tilde{p}}}} \end{bmatrix}, k_p \in \mathbb{R}, \tag{13}$$

where $\beta_{\tilde{p}}$ and $\alpha_{\tilde{q}}$ are the main coefficients of the polynomials P^2 and Q^2 respectively.

D. Crossing directions

Past results allow us to determine the values of k_p and k_d at which there exists a solution on the stability boundary. Thus, in order to determine the stability regions according to the number of unstable roots, we must make a distinction between switches (crossing towards instability) and reversals (crossing towards stability), meanwhile carry out a careful accounting of the unstable roots in each region. For such a purpose, the following result will be extremely useful.

Proposition 6: A simple root, or a pair of simple roots of the characteristic equation (6), moves from the LHP to RHP as $\mathbf{k}$ crosses a stability root boundary with $\omega \neq 0$, in the increasing direction of k_χ with $\chi \in \{p,d\}$, if:

$$S_\chi = \Re\left[\frac{s^{\eta_\chi \mu}\mathscr{E}(i\omega)}{\mathscr{D}(i\omega)}\right] > 0, \tag{14}$$

where:

$$\mathscr{E}(i\omega) = N(i\omega) + P(i\omega), \tag{15}$$

$$\mathscr{D}(i\omega) = D'(i\omega) + Q'(i\omega) + (k_p + k_d(i\omega)^\mu)\mathscr{E}'(i\omega) + k_d\mu(i\omega)^{\mu-1}\mathscr{E}(i\omega), \tag{16}$$

and where the indicative function η_χ is defined as:

$$\eta_\chi := \begin{cases} 0 & if \quad \chi = p \\ 1 & if \quad \chi = d \end{cases}. \tag{17}$$

The crossing is from the RHP to LHP, if the inequality (14) is reversed

Remark 3: As can be seen from (16), when $\omega = 0$, the crossing direction is not defined unless $\mu \geq 1$. Therefore, we cannot generally determine the stability crossing direction for the RRB.

E. Fragility Analysis

In the remaining part of this section, we will consider the *fragility problem*, which consists of computing the maximum controller parameters' deviation without loosing the closed-loop stability given by some known values $\mathbf{k}^* = (k_p^*, k_d^*)$, such that the roots of the equation $\Delta(s) = 0$ are located in $\mathbb{C}_-$. This is analogous to find the maximum parameter deviation $d \in \mathbb{R}_+$, such that the roots of stay located in $\mathbb{C}_-$ for all controllers k satisfying:

$$\sqrt{(k_p - k_p^*)^2 + (k_d - k_d^*)^2} < d. \tag{18}$$

Let us announce some notation: for a fixed $\mathbf{k}^* = (k_p^*, k_d^*)^T \in \mathbb{R}^2$ and $k(\omega) = (k_p(\omega), k_d(\omega))^T$ as in Proposition 3, introduce the function $\xi : \mathbb{R}_+ \to \mathbb{R}_+$, as:

$$\xi(\omega) := \sqrt{(k_p(\omega) - k_p^*)^2 + (k_d(\omega) - k_d^*)^2}. \tag{19}$$

We have the following:

Proposition 7: Let $\mathbf{k}^* = (k_p^*, k_d^*)^T$ be a stabilizing controller. Then, the maximum parameter deviation d of $\mathbf{k}^*$ without loosing the property of stability can be computed by:

$$d = \min\{d_\ell, d_0, d_\infty\}, \tag{20}$$

with d_ℓ, d_0 and d_∞ given by:

$$d_\ell = \min_{\omega \in \Omega_f}\{\xi(\omega)\}, \quad d_0 = \frac{a_0 + \sqrt{\alpha_0}}{b_0 + \sqrt{\beta_0}} + k_p^*, \quad d_\infty = \ell + k_d^* \tag{21}$$

where Ω_f denote the set of all roots of $f(\omega)$ defined as:

$$f(\omega) := \langle (\mathbf{k}(\omega) - \mathbf{k}^*), \frac{d\mathbf{k}(\omega)}{d\omega} \rangle, \tag{22}$$

$\langle \cdot, \cdot \rangle$ refers to the inner product and ℓ is a value that depends on the following cases

(i) $n \geq \frac{\tilde{q}}{2}$

$$\ell := \begin{cases} \frac{a_n}{b_m} & \text{if} \quad \mu + m = n \\ \frac{a_n}{\sqrt{\beta_{\tilde{p}}}} & \text{if} \quad \mu + \frac{\tilde{p}}{2} = n \\ \frac{a_n}{b_m + \sqrt{\beta_{\tilde{p}}}} & \text{if} \quad \mu + m = \mu + \frac{\tilde{p}}{2} = n \end{cases}, \tag{23}$$

(ii) $n < \frac{\tilde{q}}{2}$

$$\ell := \frac{\sqrt{\alpha_{\tilde{q}}}}{\sqrt{\tilde{\beta}_{\tilde{p}}}}. \tag{24}$$

IV. Numerical Examples

In this section, we introduce some special cases of IDTFs that illustrate the use of our results. All the closed-loop system responses presented here where computed by means of a numerical inverse Laplace transform described in [23].

A. Bessel function

The Laplace transform of the Bessel function of order zero is given by

$$H(s) = \frac{1}{\sqrt{s^2 + 1}}, \tag{25}$$

where the Bessel function of zero order $J_0(x)$ is the solution of a second order differential equation given by $x(y'' + y) + y' = 0$. We attempt to study system (25) behavior when using a fractional PD^μ controller. Then, the closed-loop system characteristic equation is described by

$$\Delta_{bessel}(s) = \sqrt{s^2 + 1} + k_p + k_d s^\mu \tag{26}$$

From Remark 1 we have $\mu \leq 1$. Propositions 4, 3 and 5 allow us to determine the crossing root boundaries as shown

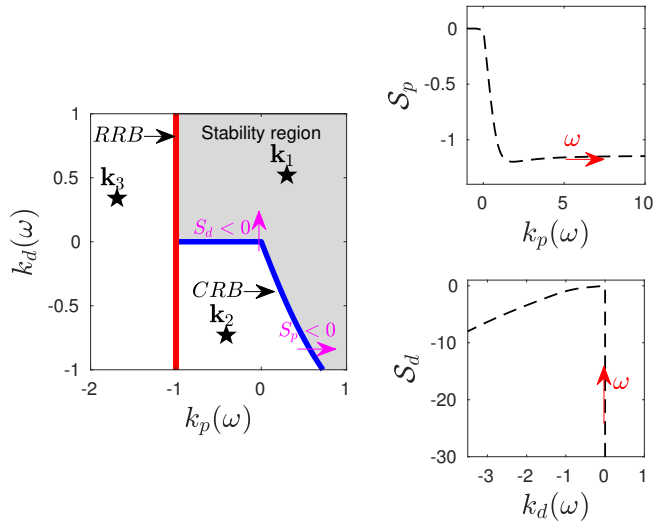

Fig. 2. The (k_p, k_d) stability region analysis (Propositions 3, 4 and 5) and the sign crossing behavior (Proposition 6).

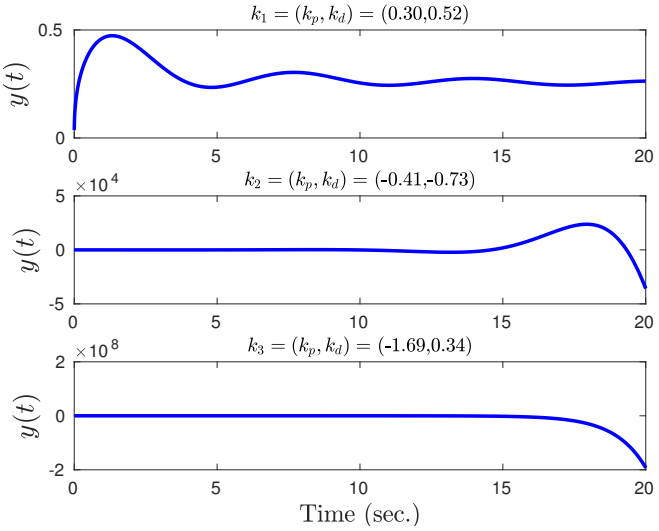

Fig. 3. Time step response of the closed-loop system with distinct controller gains. Controller gain locations are illustrated in Fig. 2.

in Fig. 2, in this case we had chosen $\mu = 0.6$. Fig. 2 shows the use of Proposition 6 by plotting (14) in the k_p and k_d direction. The value of (14) for every $\omega \neq 0$ give us a point of departure to determine the *stability region* which is shaded in gray. Finally, by choosing any (k_p, k_d) parameters inside one of the three regions enclosed by the stability root boundaries, we determined the step responses shown in Fig. 3 which show the expected responses according to the belonging region for each of the chosen (k_p, k_d).

B. First order IDTF

Consider the IDTF given by

$$H(s) = \frac{\sqrt{3s+1}}{s+\sqrt{2s+1}}, \tag{27}$$

Now, we want to implement a PD^{μ} controller to the system. We start with Propositions 5 and 4 to construct the stability

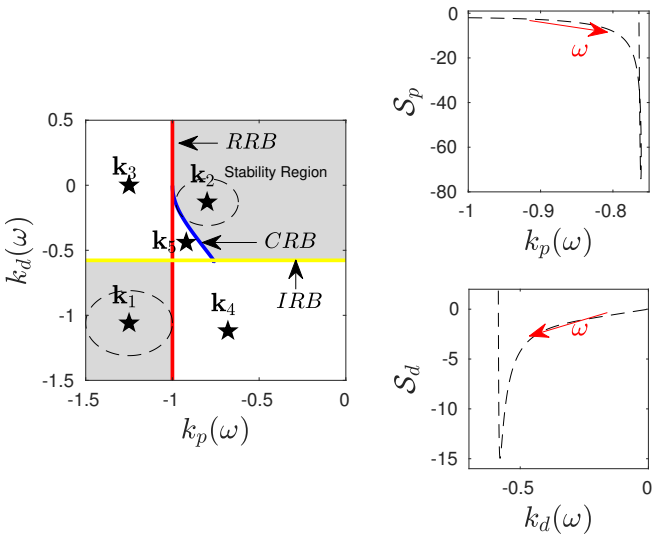

Fig. 4. The (k_p, k_d) stability region analysis (Propositions 3, 4 and 5) and the sign crossing behavior (Proposition 6).

TABLE I

Fragility Analysis

$\mathbf{k}^*$	d_0	d_∞	d_ℓ	ω	d
k_1	0.2531	0.4829	-	-	0.2531
k_2	0.2045	0.4517	0.1809	0.0686	0.1809

TABLE II

GAIN AND FRAGILITY VALUES FOR IDTF GIVEN BY EQ. 27.

root boundaries depicted in Fig. 4. A fixed $\mu = 0.3$ has been used. In this numerical example, we make use of Proposition 7 to determine the maximum parameter deviation from some arbitrarily chosen stabilizing controller gains in the stability regions shown in Fig. 4. The selected gains are k_1 and k_2 whose values and fragility are shown in Table I. Finally, to proof the behavior of the closed-loop system, we illustrate the step response in Fig. 5 for various arbitrarily chosen controller gains.

C. An infinite tree of springs and dampers

Consider the following IDTF which is used to describe a infinite tree of springs and dampers (for further details, see [3], [24]).

$$G_x(s) = \frac{\rho + \sigma s + \sqrt{(\rho+\sigma s)^2 + \varsigma s}}{ms^2 + \rho + \sigma s + \sqrt{(\rho+\sigma s)^2 + \varsigma s}}, \tag{28}$$

where $\rho = (p-1)k$, $\sigma = (q-1)b$, $\varsigma = 4(p+q-1)kb$ and $m = 2m_{last}$. Here, $p \geq 1$ is the number of springs with spring constant k, $q \geq 1$ is the number of dampers with damping constant b and m_{last} is the mass of the last element in the infinite tree [3].

The stability charts for system (28) subject to a fractional PD^{μ} controller are depicted in Fig. 6. The region are similarly found by means of Propositions 3, 4 and 5, considering the case when the parameters are: $\mu = 0.7$, $p = 2$, $q = 2$, $k = 0.2$, $b = 0.4$ and $m_{last} = 1$.

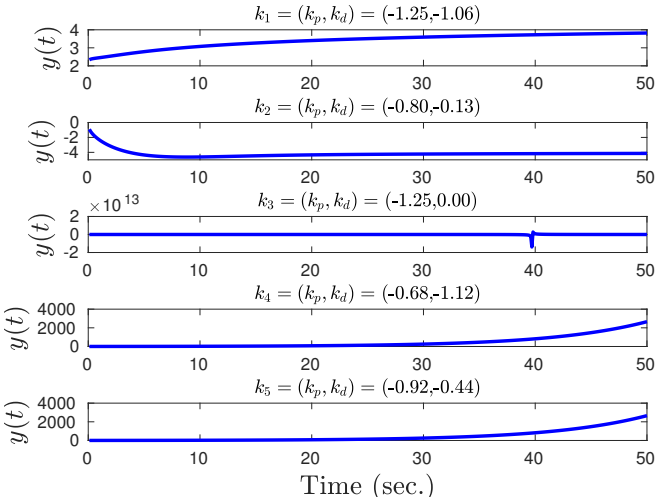

Fig. 5. Time impulse response of the closed-loop system with distinct controller gains. Controller gain locations are illustrated in Fig. 4.

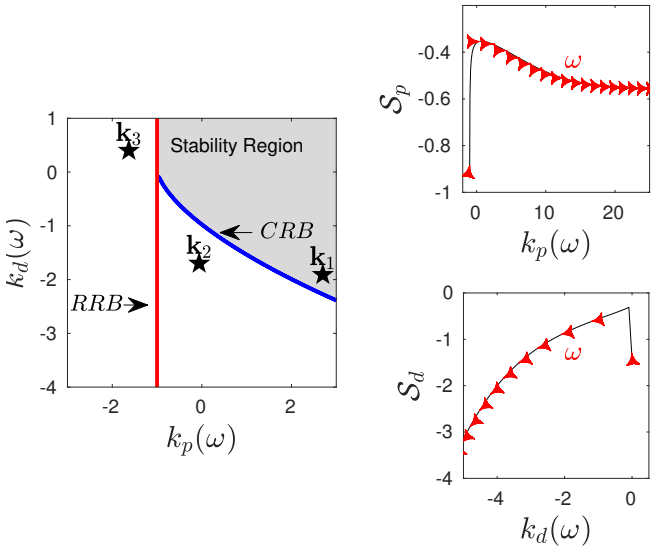

Fig. 6. The (k_p, k_d) stability region analysis (Propositions 3, 4 and 5) and the sign crossing behavior (Proposition 6). Red arrows in S_χ plots detail ω increase direction.

The stability region is detected by studying the sign of S_χ as described in Proposition 6. This enable us to find the shaded region in Fig. 6 which corresponds to the stability region. Finally, to proof the behavior of the closed-loop system, we illustrate the step response in Fig. 7 for various arbitrarily chosen controller gains.

D. Higher order IDTF

As a last example, consider the third order IDTF given by

$$H(s) = \frac{s^2 + 2s + 1 + \sqrt{2s+3}}{s^3 + 3s^2 + 4s - 2 + \sqrt{s+1}}. \tag{29}$$

By analyzing the closed-loop characteristic polynomial of system (29) subject to the fractional order PD^μ controller, we are able to find its stability region as illustrated in Fig. 8. The regions in the illustration are found by means of Propositions

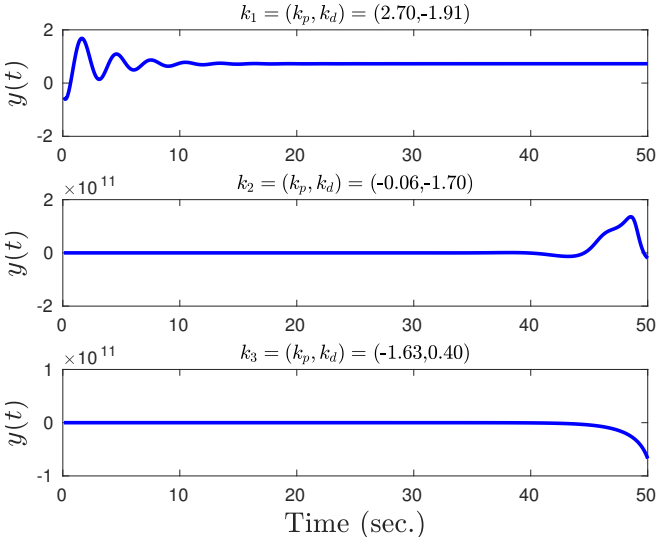

Fig. 7. Time impulse response of the closed-loop system with distinct controller gains. Controller gain locations are illustrated in Fig. 6.

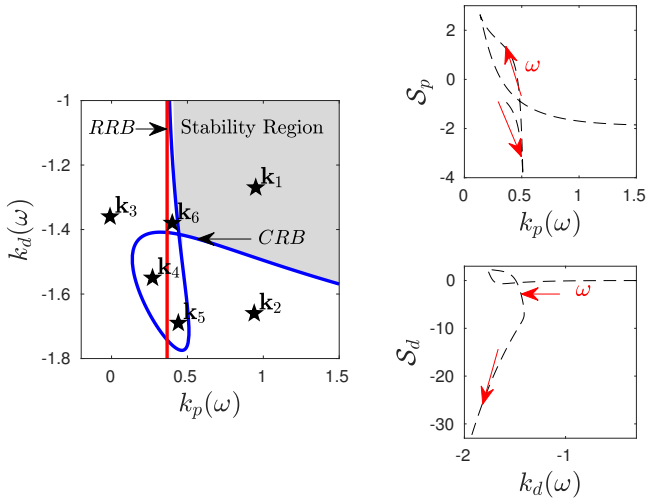

Fig. 8. The (k_p, k_d) stability region analysis (Propositions 3, 4 and 5) and the sign crossing behavior (Proposition 6).

3, 4 and 5. Here, we are considering the case when $\mu = 0.8$ to obtain such stability crossing curves.

To deterine the stability region, we have used Proposition 6. This region is depicted in Fig. 8 as the gray shaded region. As in the previous examples we have used red arrows in the S_χ plots of Fig. 8 to show the increasing direction of ω in order to study the roots crossing behavior of the closed-loop characteristic equation.

Finally, the performance of the closed-loop system is illustrated by means of its step response when using different arbitrarily chosen controller gains. We show the results of the step responses in Fig. 9.

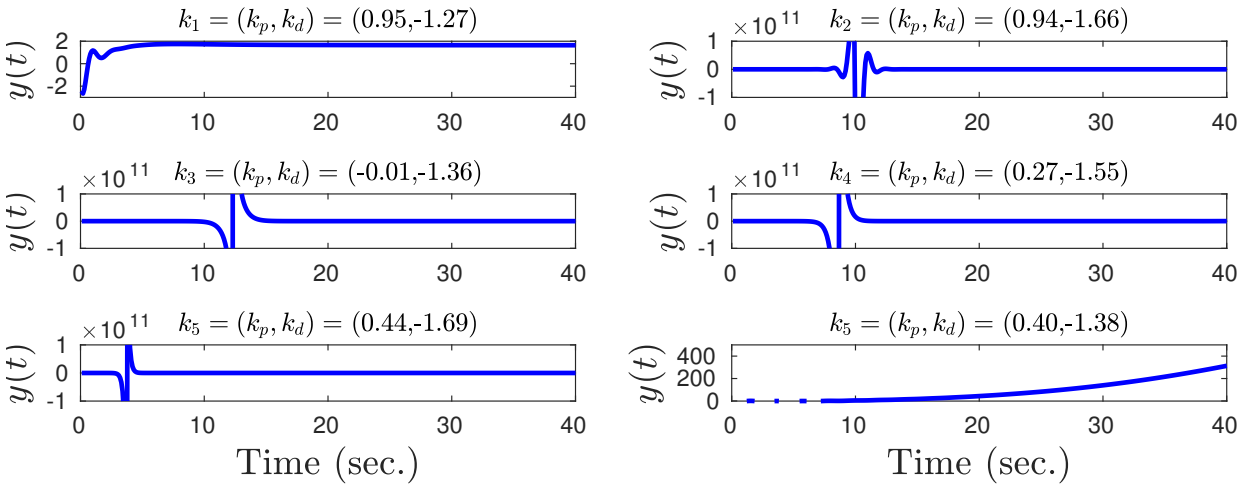

Fig. 9. Time step response of the closed-loop system with distinct controller gains. Controller gain locations are illustrated in Fig. 8.

V. Conclusions

In this work, we presented an easy methodology for finding the closed-loop stability regions on a type of IDTF being controlled by means of a fractional PD^{μ} controller. IDTFs can be found when modeling certain type of infinite order systems. Therefore, our results imply advances in controlling complex systems. The propositions we have presented were accompanied with several numerical examples. Our results can be extended to other type of multi-valued complex functions by considering the BPs stability criterion. Further research may imply the introduction of a new type of controllers which could enable us to modify the BPs' location of IDTFs.

References

[1] M. Sen, J. P. Hollkamp, F. Semperlotti, and B. Goodwine, "Implicit and fractional-derivative operators in infinite networks of integer-order components," *Chaos, Solitons & Fractals*, vol. 114, pp. 186–192, 2018.

[2] J. Mayes and M. Sen, "Approximation of potential-driven flow dynamics in large-scale self-similar tree networks," *Proceedings of the royal society a mathematical, physical and engineering sciences*, vol. 467, no. 2134, pp. 2810–2824, 2011.

[3] B. Goodwine, "Approximations for implicitly-defined dynamics of networks of simple mechanical components," in *26th Mediterranean Conference on Control and Automation*, 2018.

[4] K. Leyden, M. Sen, and B. Goodwine, "Models from an implicit operator describing a large mass-spring-damper network," *IFAC-PapersOnLine*, vol. 51, no. 2, pp. 831–836, 2018.

[5] R. F. Curtain and H. Zwart, *An Introduction to Infinite-Dimensional Linear Systems Theory*, S.-V. B. Heidelberg, Ed. Texts in Applied Mathematics, 1995, vol. 21.

[6] R. F. Curtain, *A Synthesis of Time and Frequency Domain Methods for the Control of Infinite-Dimensional Systems: A System Theoretic Approach*. Frontiers in Applied Mathematics, 1992, ch. 5, pp. 171–223.

[7] D. Hernandez-Herran, M. Núñez López, and J. Velasco-Hernandez, "Telegraphic double porosity models for head transient behavior in naturally fractured aquifers," *Water Resour. Res.*, vol. 49, pp. 4399–4408, 2013.

[8] Y.-S. Wu, C. A. Ehlig-Economides, G. Qin, Z. Kang, W. Zhang, B. T. Ajayi, and Q. Tao, "A triple-continuum pressure-transient model for a naturally fractured vuggy reservoir," in *SPE Annual Technical Conference and Exhibition*, 2007.

[9] C. R. Knospe, "PID control," *IEEE Control Systems*, vol. 26, no. 1, pp. 30–31, 2006.

[10] P. Shah and S. Agashe, "Review of fractional PID controller," *Mechatronics*, vol. 38, pp. 29–41, 2016.

[11] A. Tepljakov, E. Petlenkov, J. Belikov, and M. Halás, "Design and implementation of fractional-order PID controllers for a fluid tank system," in *2013 American Control Conference (ACC), Washington DC, USA*, 2013.

[12] A.-J. Guel-Cortez, C.-F. Méndez-Barrios, J. Romero, V. Ramírez-Rivera, and E. González-Galván, "Fractional$-PD^{\mu}$ controllers design for lti-systems with time-delay. a geometric approach," in *2018-5th International Conference on Control, Decision and Information Technologies*, 2018.

[13] A. J. Guel-Cortez, C.-F. Mndez-Barrios, E. J. Gonzlez-Galvn, G. Meja-Rodrguez, and L. Flix, "Geometrical design of fractional PD^{μ} controllers for linear time-invariant fractional-order systems with time delay," *Proceedings of the Institution of Mechanical Engineers, Part I: Journal of Systems and Control Engineering*, 2019.

[14] R. Caponetto, *Fractional Order Systems: Modeling and Control Applications*, ser. World Scientific Series on Nonlinear Science: Series A. World Scientific, 2010.

[15] C. Monje, Y. Chen, B. Vinagre, D. Xue, and V. Feliu-Batlle, *Fractional-order Systems and Controls: Fundamentals and Applications*, ser. Advances in Industrial Control. Springer London, 2010.

[16] M. S. Tavazoei, "From traditional to fractional PI control: A key for generalization," *IEEE Industrial Electronics Magazine*, vol. 6, no. 3, pp. 41–51, Sept 2012.

[17] D. Valério and J. S. da Costa, *An Introduction to Fractional Control*, ser. Control, Robotics and Sensors Series. Institution of Engineering and Technology, 2013.

[18] E. N. Gryazina, B. T. Polyak, and A. A. Tremba, "D-decomposition technique state-of-the-art," *Automation and Remote Control*, vol. 69, no. 12, pp. 1991–2026, 2008.

[19] E. N. Gryazina, "The d-decomposition theory," *Automation and Remote Control*, vol. 65, no. 12, pp. 1872–1884, 2004.

[20] H. Cohen, *Complex analysis with application in science and engineering*. Springer, 2007.

[21] T. Needham, *Visual Complex Analysis*. Clarendon Press, Oxford, 1997.

[22] F. Merrikh-Bayat and M. Karimi-Ghartemani, "On the essential instabilities caused by fractional-order transfer functions," *Mathematical Problems in Engineering*, 2008.

[23] J. Abate and W. Whitt, "A unified framework for numerically inverting laplace transforms," *INFORMS Journal on Computing*, vol. 18, no. 4, pp. 408–421, 2006.

[24] A.-J. Guel-Cortez, M. Sen, and B. Goodwine, "Closed form time response of an infinite tree of mechanical components described by an irrational transfer function," in *2019 American Control Conference*, Philadelphia Marriott Downtown Philadelphia, Pennsylvania United States, July 2019, to be published.